Iron Particles Enhance Visualization of Experimental Gliomas with High-Resolution Sonography

Ingo Nolte, Giles H. Vince, Mathias Maurer, Christian Herbold, Roland Goldbrunner, Laszlo Solymosi, Guido Stoll and Martin Bendszus

AJNR Am J Neuroradiol 2005, 26 (6) 1469-1474
http://www.ajnr.org/content/26/6/1469

AJNR Am J Neuroradiol 26:1469–1474, June/July 2005

Iron Particles Enhance Visualization of Experimental Gliomas with High-Resolution Sonography

Ingo Nolte, Giles H. Vince, Mathias Maurer, Christian Herbold, Roland Goldbrunner, Laszlo Solymosi, Guido Stoll, and Martin Bendszus

BACKGROUND AND PURPOSE: **Intraoperative MR imaging and sonography are used for navigation during neurosurgical procedures. The purpose of this experimental study was to evaluate the potential of high-resolution sonography using superparamagnetic iron oxide (SPIO) particles as a contrast medium to delineate brain tumors and to relate these findings with those of MR imaging.**

METHODS: **C6 gliomas were implanted in 36 rats. Eleven days after tumor implantation, the animals underwent MR imaging with a 1.5-T MR imaging unit. Twelve animals received gadopentetate dimeglumine immediately before the MR examination, 12 animals were injected with SPIO particles 24 hours before MR imaging, and 12 animals received no contrast agent. Immediately after MR imaging, the animals were sacrificed and their brains were removed and placed in saline. Sonography was performed instantly after brain removal. Brains were embedded in paraffin, and sections were stained for iron with Perl's stain and for macrophages with ED-1 immunohistochemistry.**

RESULTS: **At MR imaging, the tumors appeared hyperintense on T2-weighted and gadolinium-enhanced T1-weighted images. After application of SPIO particles, they became markedly hypointense on T2-weighted images and hypo- to hyperintense on T1-weighted images. On sonograms, gliomas were iso- to slightly hyperechoic to normal brain parenchyma on nonenhanced and on gadolinium-enhanced images. After application of SPIO particles, tumors became markedly hyperechoic and were distinctly demarcated from the surrounding brain tissue.**

CONCLUSION: **SPIO particles improved the detection and demarcation of the experimental gliomas on sonograms, which may improve intraoperative neuronavigation with sonography.**

The treatment of choice for malignant gliomas is tumor resection followed by adjuvant radiation therapy and/or chemotherapy. The extent of surgical tumor removal has an effect on tumor regrowth and patient prognosis (1). Intraoperative MR imaging has been shown to reduce the amount of residual tumor tissue in glioblastomas (2). Several clinical studies also report on the value of sonography in the intraoperative resection control of brain tumors (3–5). In addition, residual tumor mass delineated by sonography correlates with postoperative survival of patients with high-grade gliomas (6). In general, brain tumors are slightly hyperechoic on intraoperative sonograms; however, in a substantial number of cases the tumor margins are poorly defined on sonograms (4, 5). Superparamagnetic iron oxide (SPIO) particles have been shown to accumulate both in experimental as well as in human gliomas (7, 8). Our purpose was to evaluate the potential of high-resolution sonography using SPIO particles as a contrast medium to delineate brain tumors and to relate these findings with those of MR imaging.

Received August 31, 2004; accepted after revision October 20.

From the Departments of Neuroradiology (I.N., L.S., M.B.), Neurosurgery (G.H.V., C.H., R.G.), and Neurology (I.N., M.M., G.S.), University of Würzburg, Germany.

M.B. is a stiftungs professor supported by a grant from Schering Deutschland GmbH, Berlin. I.N. is supported by a grant from the faculty of clinical medicine, Mannheim.

Address reprint requests to Martin Bendszus, MD, Department of Neuroradiology, University of Würzburg, Josef-Schneider-Str.11, D-97080 Würzburg, Germany.

Methods

Tumor Implantation

The C6 rat glioma cell line was purchased from the American Type Culture Collection (Rockville, MD). Clones were grown as a monolayer in 75-mL flasks in Dulbecco's minimum essential medium supplemented with 10% fetal calf serum

(Flow Laboratories), 100 U/mL penicillin, and 100 mg/mL streptomycin (Flow Laboratories). Cells were grown at 37°C, 5.0% CO_2, and 100% humidity. Reaggregations of *in vitro* monolayer tumor cells (spheroids) were produced by seeding 5×106 cells into a 75-mL flask that had been coated previously with 1.0% Noble agar (Difco, Detroit, MI) covered by a liquid medium overlay (9). Spheroids were screened for signs of necrosis by using inverted light microscopy to avoid confusion of *in vitro* tumor necrosis with *in vivo* tumor necrosis (*in vivo*, the spheroid can recruit tumor vessels and can thereby grow to a larger size before necrosis occurs [9]). Necrotic centers were observed when a diameter of more than 400–500 μm was reached. After 5 days, spheroids of each clone with a diameter of 400 μm and without a necrotic core were selected for implantation.

All experimental procedures were approved by the animal care committee of the University of Würzburg and in accordance with the State of Bavaria guidelines for the care of laboratory animals. The hosts were 36 male Sprague-Dawley rats weighing 300–350 g. They were kept on a regular daylight schedule with rodent animal chow and water ad libidum. For implantation surgery, each animal was deeply anesthetized with an intramuscular application of ketamine 100 mg/kg (Ketanest; Parke-Davis, Morris Plains, NJ) and xylazine 10 mg/kg (Rompun; Bayer Vital, Leverkusen, Germany). The head was mounted in a headholder, and a midline skin incision was performed. The skull was trephined at the bregma, and the dura was exposed. The dura was then excised around the bone under microscopic control to prevent vascularization by dural vessels. The pia and the cortex were incised in an X shape with a microscalpel. A single spheroid was then placed subcortically into the X-shaped incision.

MR Imaging Measurements

All measurements were performed with a 1.5-T unit (Vision; Siemens, Erlangen, Germany) by using a round surface coil (diameter 4 cm). Animals were deeply anesthetized with an intramuscular application of ketamine 100 mg/kg (Ketanest; Parke-Davis) and xylazine 10 mg/kg (Rompun; Bayer Vital). In 12 animals, gadopentetate dimeglumine 0.2 mL/kg (Magnevist; Schering, Berlin, Germany) was injected before the MR examination. Twelve animals had received SPIO particles (Resovist 300 μmol/kg of body weight; Schering) 24 hours before imaging, and 12 animals received no contrast agent. SPIO particles are mostly taken up by the reticuloendothelial sytem of liver and spleen (10) and are therefore mainly used for hepatic imaging. A minor portion is taken up by circulating macrophages that subsequently leave the circulation and can be visualized with MR imaging because of their strong paramagnetic effect (11). The MR protocol consisted of T2-weighted (2500/96 TR/TE) and T1-weighted (600/14) turbo spin-echo sequences in the coronal plane (60-mm FOV, 3-mm section thickness). The section position was perpendicular to the skull base.

Sonography

After the MR examinations, animals were euthanized by intracardiac injection of pentobarbital 50 mg/kg under deep ketamin anesthesia. The brains were rapidly and carefully removed and placed into a water tank on a navigable mechanical table. Sonography was performed *ex vivo* by using a color-coded, phased-array sonographic system (Sonoline Elegra; Siemens) equipped with a VX 13.5 13-MHz transducer with an emission frequency of 12 MHz. The axial resolution in the focus zone is about 0.7 mm. The sonographic system indexes chosen were penetration depth 1.5 cm, dynamic range 60 dB, low persistence, focus length 1 cm. Image brightness and gain (26 dB) were not changed for sonification of the different groups. The sonographic transducer was fixed directly above the brain, which was imaged in coronal and sagittal planes by continuously moving the tank with the mechanical table.

Histologic Examination

Brains were immersed in 4% paraformaldehyde and embedded in paraffin. Then, 10-μm coronal sections were cut through the cortical hemispheres and stained with Perl's stain for iron detection and either counterstained with hematoxylin-eosin or, in addition, stained for macrophages by immunohistochemistry by using the monoclonal antibody ED-1, as described in detail elsewhere (12).

Results

Both on sonograms and MR images, the tumors appeared round to ellipsoid (Fig 1). Imaging characteristics are summarized in the Table. On nonenhanced MR images, the tumors were isointense on T1-weighted images and predominantly hyperintense on T2-weighted images, whereas on sonograms they were slightly hyperechoic to the surrounding brain parenchyma. After application of gadopentetate dimeglumine, the lesions revealed a marked contrast enhancement. On T2-weighted MR images and sonograms, the signal intensity and echogenicity, respectively, were unchanged compared with that on nonenhanced images. Twenty-four hours after systemic SPIO application, the tumors revealed a predominant hypointensity on T2-weighted images and a mixed hypo- to hyperintensity on T1-weighted images. On sonograms, the application of SPIO particles markedly increased tumor hyperechogenicity. This was most pronounced at the tumor margins where the glioma was sharply demarcated from the surrounding brain tissue. Two brains underwent additional histologic analysis. After Perl's stain, islets of blue iron-positive cells with the typical morphology of tumor cells were detectable within the tumor parenchyma (Fig 2, A). In addition, small iron-positive cells were found diffusely within the tumors, and more prominently at their margins (Fig 2B). Most of these scattered iron-positive cells could be identified as ED-1–positive macrophages by double labeling (Fig 2C and 2D).

Discussion

Intraoperative neuronavigation and image-guided resection control have gained importance during the past years. The most commonly applied intraoperative imaging modalities include MR imaging and sonography. In the present study, we compared the imaging characteristics of experimental glioma with different imaging modalities (nonenhanced MR imaging and sonography, gadolinium-enhanced MR imaging and sonography, SPIO-enhanced MR imaging and sonography) in order to compare tumor visualization and demarcation of the tumor edges.

As a principal and novel finding, we have shown that SPIO administration increases tumor echogenicity on sonograms. On nonenhanced sonograms, gliomas have been reported to appear iso- to hyperechoic

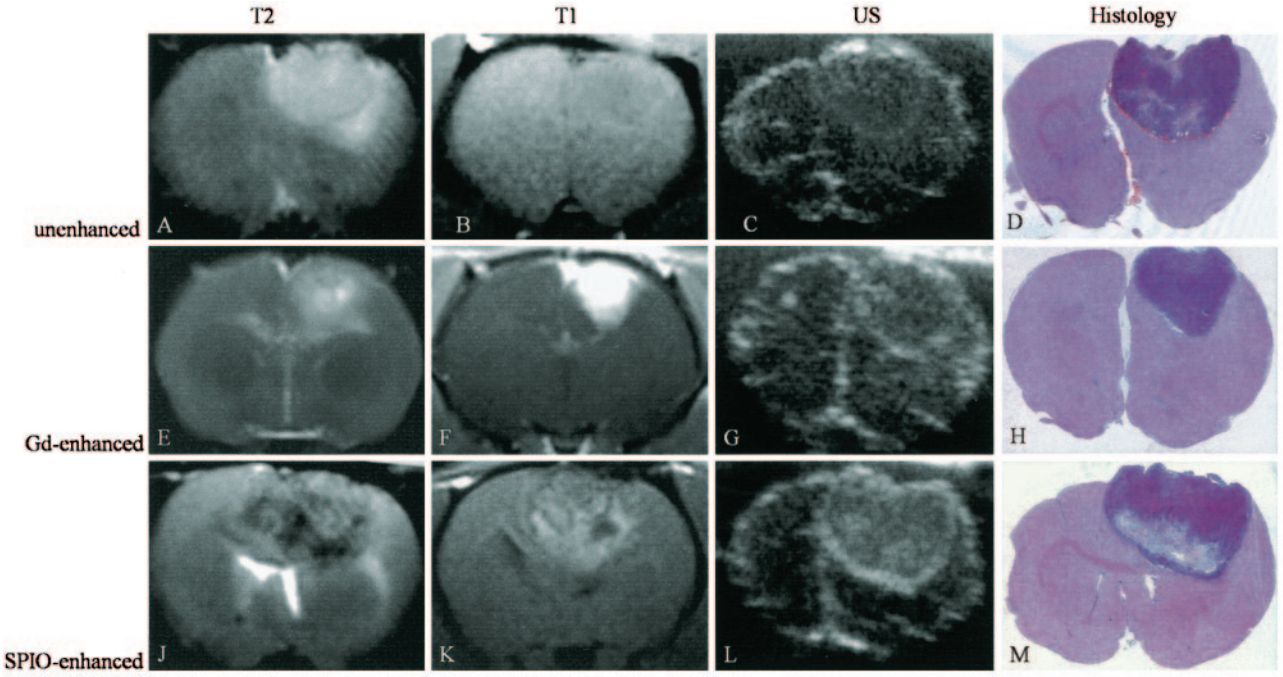

FIG 1. *A–M*, MR images (T2-weighted, 2500/96; T1-weighted, 600/14), sonograms (*US*), and photomicrographs of paraffin sections (hematoxylin-eosin stain; original magnification, X2) of C6 glioma in rat brain. Each row shows the different modalities in one animal. Images in the first row (*A–D*) were obtained without contrast media, the second row of images (*E–H*) was gadolinium-enhanced, and images in the third row (*J–M*) were SPIO-enhanced.

A–D, On the nonenhanced images, the C6 glioma is predominantly hyperintense on the T2-weighted image (*A*) and isointense on the T1-weighted image (*B*). On the sonogram (*C*), the tumor appears iso- to slightly hyperechoic to brain tissue. With hematoxylin-eosin staining (*D*), the corresponding area is clearly identifiable.

E–H, After injection of gadopentetate dimeglumine, the tumor is hyperintense on the T1-weighted image (*F*) and reveals similar characteristics on T2-weighted image (*E*), sonogram (*G*), and hematoxylin-eosin staining (*H*) to those of the tumor on nonenhanced images.

J–M, Twenty-four hours after injection of SPIO particles, the tumor is inhomogeneously hypo- to hyperintense on T2-weighted (*J*) and T1-weighted (*K*) images. On the sonogram (*L*), the tumor appears inhomogeneously hyperechoic to brain tissue with hyperechogic margins.

Imaging characteristics of the 36 experimental gliomas

Contrast Agent	Hyperechogenicity on Sonogram*			Size of Tumor on Sonogram (cm^2)†	Hypointensity on T2-Weighted MR Image*		
	−	+	++		−	+	++
SPIO particles (n = 12)	1	3	8	0.11 ± 0.06	1	6	5
Gadopentetate dimeglumine (n = 12)	9	3	0	0.18 ± 0.1	12	0	0
None (n = 12)	9	2	1	0.15 ± 0.08	12	0	0

Note.—The − indicates absent; +, moderate; ++, extensive

* Data are number of tumors.

† Data are mean ± SD. Tumor size on sonogram was measured as maximal coronal area.

(3, 4, 13) to the surrounding brain tissue. Especially on intraoperative sonograms, tumor demarcation can be difficult because blood clots in the resection cavity and superimposing tissue margins may also be slightly hyperechoic (5). Moreover, tumor echogenicity may not differ significantly from that of surrounding normal brain tissue (3, 4).

Intraoperative MR imaging has been shown to increase the extent of tumor resection in patients with high-grade glioma (14). Nevertheless, intraoperative imaging has several limitations including brain shift (15–18) and surgically induced extravasation of gadolinium-based contrast agents, potentially mimicking residual tumor (19, 20). Ultrasmall iron oxide particles have been suggested as a possible solution for the latter problem since they are applied preoperatively and are already cleared from the blood pool at the time of surgery (21).

Previous experimental and clinical studies have shown an increase of tissue echogenicity due to local iron deposition. Stereotactically injected FeCl3 into rat substantia nigra causes hyperechogenicity (22). In a postmortem brain analysis of 20 patients without extrapyramidal disorders, hyperechogenicity of the substantia nigra on sonograms was related to a higher tissue iron level (23). The change of impedance is generally accepted as the mechanism of iron-induced hyperechogenicity, though additional effects such as

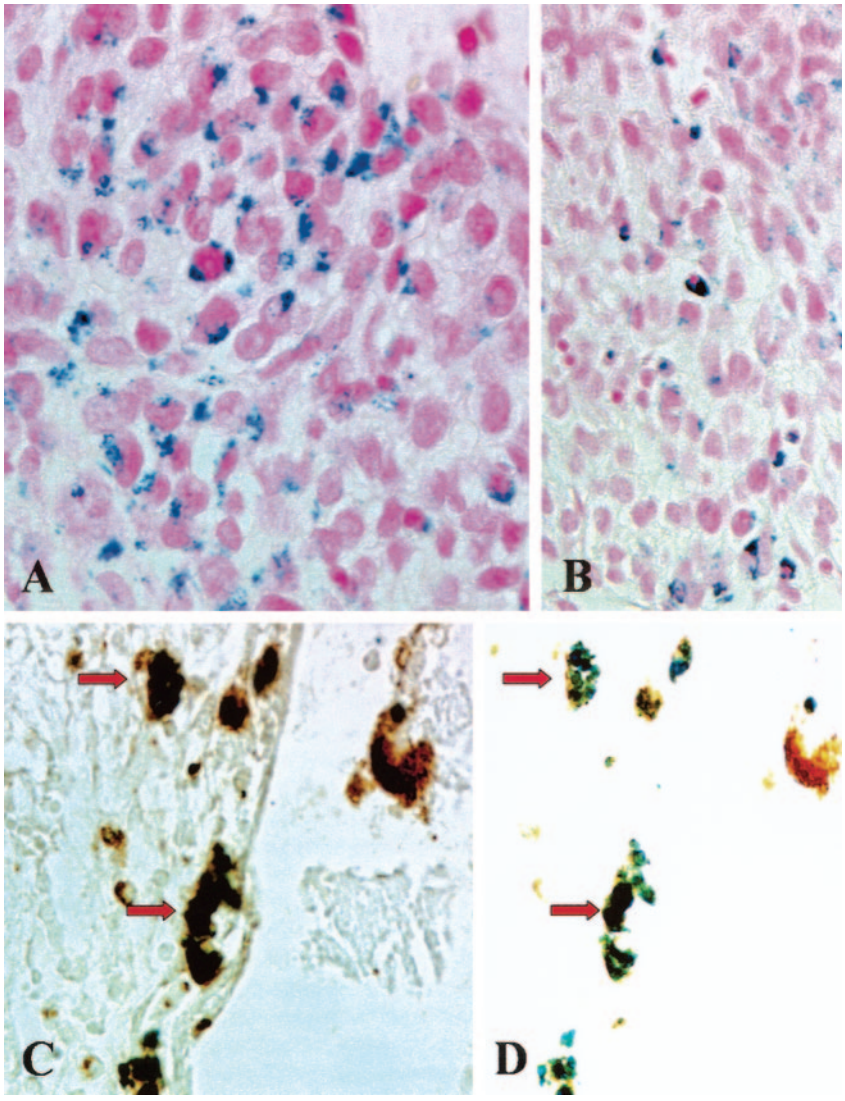

FIG 2. *A–D*, Histologic and immunohistologic localization of iron, tumor cells, and macrophages. Photomicrographs (original magnification, X500 [*A*, *C*, and *D*] and X330 [*B*]) of paraffin sections stained with Perl's stain (*A* and *B*) for detection of SPIO particles show iron-laden tumor cells in the center of the tumor in *A* and mostly mononuclear cells in the periphery of the tumor in *B*. These cells represent iron-labeled macrophages as shown by double labeling with the antibody ED-1 (*C*). The black-appearing (due to overlap of blue and brown staining product) macrophages in *C* show discernible blue staining for iron and brown ED-1 immunoreactivity in *D* when the same section is examined by using a different optic filter of the microscope (identical cells are marked by arrows).

the specific molecular environment may play a role as well, as ferritin does not show a comparable hyperechogenic effect (22).

Uptake of iron particles in experimental and human glioma (7, 8, 24–28) has already been demonstrated both on MR images and at histologic examination. In the view of these previous findings, we tested the effect of systemic iron particle application on tumor echogenicity on sonograms. Administration of iron particles induced an increase of echogenicity on sonograms compared with nonenhanced sonograms, thereby demarcating the tumor margins from the surrounding brain tissue. In a clinical setting, sonography may assist in tumor resection.

Even though the increase in tumor visualization on sonograms was obvious, some potential limitations have to be considered. In the present study, we have shown that iron particles can be used to enhance echogenicity on sonograms in a rat brain tumor model. However, the C6 glioma model—although one of the most recognized models for human glioblastoma—does not adequately reflect the infiltrating nature of the human glioblastoma. Because of this limitation, we were not able to prove that SPIO particles can be used to delineate infiltrating glioma cells. Nevertheless, Varallyay et al (7) and Enochs et al (29) reported that infiltrating human glioma could effectively be labeled by iron particles as shown on MR images.

Second, controversy appears in the literature regarding the specific type of cell within the tumor that takes up the iron particles. Zimmer et al (8, 24) reported *in vivo* uptake of monocrystalline iron oxide nanoparticles (MIONs) exclusively in gliosarcoma cells. Moore et al (25) quantified *in vivo* MION uptake in GFP-expressing 9L glioma and found labeled MION to be co-localized predominantly with GFP-expressing tumor cells and, to a lesser degree, within tumor-associated macrophages and tumor vascular endothelium. Fleige et al (28) used labeled ultrasmall SPIO in GFP-expressing F98 glioma cells *in vivo* and detected the ultrasmall SPIO predominantly in microglia and macrophages but hardly in tumor cells. Varallyay et al (7) applied ferrumoxtran in 17 patients with different histologic types of brain tumors and found tumor iron enhancement in 15 cases. In one

patient with an anaplastic oligodendroglioma, histologic work-up revealed most iron staining in cells with astrocytic morphology and, to a lesser degree, in tumor cells. In our study, accumulation of systemically applied SPIO particles occurred in both tumor cells and macrophages, with the latter predominantly located at the tumor margins. Tumor cells could be identified on the basis of their typical morphology, and macrophages by double labeling with the monoclonal antibody ED-1. Therefore, we believe that the capsule-like appearance on SPIO-enhanced sonograms is due to iron particles within macrophages. Uptake of SPIO particles in macrophages is consistent with our previous findings in neurodegeneration, cerebral ischemia, and autoimmune disorders of the nervous system (12, 30, 31). Most important, we could show that the presence of iron-laden macrophages in these neurologic disorders reflected recent infiltration from the circulation into the nervous system, whereas resident macrophages/microglia were not labeled. Although tumor cells clearly must have taken up SPIO particles locally within the brain, it is very likely that iron-laden macrophages represent an acute inflammatory response from the circulation. Thus, at the present stage, sensitivity and specificity of iron enhancement is limited, a problem well known from nonenhanced and contrast-enhanced CT and MR imaging (32–36); however, as proof of principle we were able to show that SPIO particles improve the detection and demarcation of experimental glioma on sonograms.

Moreover, detection of iron particles on MR images is also possible in extracerebral human tumor cell lines (breast carcinoma, colon carcinoma, and small lung cell carcinoma [25]). Our results imply that SPIO particles may also improve sonographic delineation in extracerebral tumors that show SPIO-enhancement on MR images.

More experimental data are needed to exactly clarify the mechanism of iron uptake in tumor cells and macrophages in glioma before a clinical application can be considered.

Conclusion

The intravenous injection of SPIO particles improved the detection and demarcation of experimental gliomas on sonograms. This finding may assist intraoperative neuronavigation with sonography.

References

1. Albert FK, Forsting M, Sartor K, Adams HP, Kunze S. **Early postoperative magnetic resonance imaging after resection of malignant glioma: objective evaluation of residual tumor and its influence on regrowth and prognosis.** *Neurosurgery* 1994;34:45–60; discussion 60–61
2. Wirtz CR, Knauth M, Staubert A, et al. **Clinical evaluation and follow-up results for intraoperative magnetic resonance imaging in neurosurgery.** *Neurosurgery* 2000;46:1112–1120; discussion 1120–1122
3. Hammoud MA, Ligon BL, elSouki R, Shi WM, Schomer DF, Sawaya R. **Use of intraoperative ultrasound for localizing tumors and determining the extent of resection: a comparative study with magnetic resonance imaging.** *J Neurosurg* 1996;84:737–741
4. Le Roux PD, Berger MS, Wang K, Mack LA, Ojemann GA. **Low grade gliomas: comparison of intraoperative ultrasound characteristics with preoperative imaging studies.** *J Neurooncol* 1992;13:189–198
5. Chacko AG, Kumar NK, Chacko G, Athyal R, Rajshekhar V. **Intraoperative ultrasound in determining the extent of resection of parenchymal brain tumours: a comparative study with computed tomography and histopathology.** Acta Neurochir (Wien) 2003;145:743–748; discussion 748
6. Maurer M, Becker G, Wagner R, et al. **Early postoperative transcranial sonography (TCS), CT, and MRI after resection of high grade glioma: evaluation of residual tumour and its influence on prognosis.** *Acta Neurochir* (Wien) 2000;142:1089–1097
7. Varallyay P, Nesbit G, Muldoon LL, et al. **Comparison of two superparamagnetic viral-sized iron oxide particles ferumoxides and ferumoxtran-10 with a gadolinium chelate in imaging intracranial tumors.** *AJNR Am J Neuroradiol* 2002;23:510–519
8. Zimmer C, Weissleder R, Poss K, Bogdanova A, Wright SC Jr, Enochs WS. **MR imaging of phagocytosis in experimental gliomas.** *Radiology* 1995;197:533–538
9. Goldbrunner RH, Wagner S, Roosen K, Tonn JC. **Models for assessment of angiogenesis in gliomas.** *J Neurooncol* 2000;50:53–62
10. Hamm B, Staks T, Taupitz M, et al. **Contrast-enhanced MR imaging of liver and spleen: first experience in humans with a new superparamagnetic iron oxide.** *J Magn Reson Imaging* 1994;4:659–668
11. Chen F, Ward J, Robinson PJ. **MR imaging of the liver and spleen: a comparison of the effects on signal intensity of two superparamagnetic iron oxide agents.** *Magn Reson Imaging* 1999;17:549–556
12. Bendszus M, Stoll G. **Caught in the act: in vivo mapping of macrophage infiltration in nerve injury by magnetic resonance imaging.** *J Neurosci* 2003;23:10892–10896
13. Enzmann DR, Wheat R, Marshall WH, et al. **Tumors of the central nervous system studied by computed tomography and ultrasound.** *Radiology* 1985;154:393–399
14. Knauth M, Wirtz CR, Tronnier VM, Aras N, Kunze S, Sartor K. **Intraoperative MR imaging increases the extent of tumor resection in patients with high-grade gliomas.** *AJNR Am J Neuroradiol* 1999;20:1642–1646
15. Kelly PJ, Earnest F 4th, Kall BA, Goerss SJ, Scheithauer B. **Surgical options for patients with deep-seated brain tumors: computer-assisted stereotactic biopsy.** *Mayo Clin Proc* 1985;60:223–229
16. Kelly PJ, Kall BA, Goerss S, Earnest F. **Present and future developments of stereotactic technology.** *Appl Neurophysiol* 1985;48:1–6
17. Kelly PJ, Kall BA, Goerss S, Earnest F 4th. **Computer-assisted stereotaxic laser resection of intra-axial brain neoplasms.** *J Neurosurg* 1986;64:427–439
18. Nimsky C, Ganslandt O, Cerny S, Hastreiter P, Greiner G, Fahlbusch R. **Quantification of, visualization of, and compensation for brain shift using intraoperative magnetic resonance imaging.** *Neurosurgery* 2000;47:1070–1079; discussion 1079–1080
19. Knauth M, Aras N, Wirtz CR, Dorfler A, Engelhorn T, Sartor K. **Surgically induced intracranial contrast enhancement: potential source of diagnostic error in intraoperative MR imaging.** *AJNR Am J Neuroradiol* 1999;20:1547–1553
20. Dietrich J, Schneider JP, Schulz T, Seifert V, Trantakis C, Kellermann S. **Appearance of the resection area of brain tumors in intraoperative MRI imaging.** *Radiologe* 1998;38:935–942
21. Knauth M, Egelhof T, Roth SU, Wirtz CR, Sartor K. **Monocrystalline iron oxide nanoparticles: possible solution to the problem of surgically induced intracranial contrast enhancement in intraoperative MR imaging.** *AJNR Am J Neuroradiol* 2001;22:99–102
22. Berg D, Grote C, Rausch WD, et al. **Iron accumulation in the substantia nigra in rats visualized by ultrasound.** *Ultrasound Med Biol* 1999;25:901–904
23. Berg D, Roggendorf W, Schroder U, et al. **Echogenicity of the substantia nigra: association with increased iron content and marker for susceptibility to nigrostriatal injury.** *Arch Neurol* 2002;59:999–1005
24. Zimmer C, Wright SC Jr, Engelhardt RT, et al. **Tumor cell endocytosis imaging facilitates delineation of the glioma-brain interface.** *Exp Neurol* 1997;143:61–69
25. Moore A, Marecos E, Bogdanov A Jr, Weissleder R. **Tumoral distribution of long-circulating dextran-coated iron oxide nanoparticles in a rodent model.** *Radiology* 2000;214:568–574
26. Moore A, Marecos E, Simonova M, Weissleder R, Bogdanov A Jr. **Novel gliosarcoma cell line expressing green fluorescent protein: a model for quantitative assessment of angiogenesis.** *Microvasc Res* 1998;56:145–153
27. Moore A, Weissleder R, Bogdanov A Jr. **Uptake of dextran-coated monocrystalline iron oxides in tumor cells and macrophages.** *J Magn Reson Imaging* 1997;7:1140–1145

28. Fleige G, Nolte C, Synowitz M, Seeberger F, Kettenmann H, Zimmer C. **Magnetic labeling of activated microglia in experimental gliomas.** *Neoplasia* 2001;3:489–499
29. Enochs WS, Harsh G, Hochberg F, Weissleder R. **Improved delineation of human brain tumors on MR images using a long-circulating, superparamagnetic iron oxide agent.** *J Magn Reson Imaging* 1999;9:228–232
30. Kleinschnitz C, Bendszus M, Frank M, Solymosi L, Toyka KV, Stoll G. **In vivo monitoring of macrophage infiltration in experimental ischemic brain lesions by magnetic resonance imaging.** *J Cereb Blood Flow Metab* 2003;23:1356–1361
31. Stoll G, Wesemeier C, Gold R, Solymosi L, Toyka KV, Bendszus M. **In vivo monitoring of macrophage infiltration in experimental autoimmune neuritis by magnetic resonance imaging.** *J Neuroimmunol* 2004;149:142–146
32. Shaw EG, Scheithauer BW, O'Fallon JR, Tazelaar HD, Davis DH. **Oligodendrogliomas: the Mayo Clinic experience.** *J Neurosurg* 1992;76:428–434
33. Vonofakos D, Marcu H, Hacker H. **Oligodendrogliomas: CT patterns with emphasis on features indicating malignancy.** *J Comput Assist Tomogr* 1979;3:783–788
34. Daumas-Duport C, Tucker ML, Kolles H, et al. **Oligodendrogliomas, II: a new grading system based on morphological and imaging criteria.** *J Neurooncol* 1997;34:61–78
35. Barker FG 2nd, Chang SM, Huhn SL, et al. **Age and the risk of anaplasia in magnetic resonance-nonenhancing supratentorial cerebral tumors.** *Cancer* 1997;80:936–941
36. Scott JN, Brasher PM, Sevick RJ, Rewcastle NB, Forsyth PA. **How often are nonenhancing supratentorial gliomas malignant? A population study.** *Neurology* 2002;59:947–949